

X-ray Emission Spectroscopy of Cerium Across the γ - α Volume Collapse Transition

M. J. Lipp,¹ A. P. Sorini,^{1,2} J. Bradley,^{1,*} B. Maddox,¹ K. T. Moore,¹ H. Cynn,¹ T. P. Devereaux,^{2,3}
Y. Xiao,⁴ P. Chow,⁴ and W. J. Evans¹

¹Lawrence Livermore National Laboratory, Livermore, California 94550, USA

²Stanford Institute for Materials and Energy Sciences, SLAC National Accelerator Laboratory and Stanford University, Menlo Park, California 94305, USA

³Geballe Laboratory for Advanced Materials, Stanford University, Stanford, California 94305, USA

⁴HPCAT, Carnegie Institute of Washington, Argonne, Illinois 60439, USA

(Received 27 July 2012; published 9 November 2012)

High-pressure x-ray emission measurements are used to provide crucial evidence in the longstanding debate over the nature of the isostructural (α , γ) volume collapse in elemental cerium. Extended local atomic model calculations show that the satellite of the $L\gamma$ emission line offers direct access to the total angular momentum observable $\langle J^2 \rangle$. This satellite experiences a 30% steplike decrease across the volume collapse, validating the Kondo model in conjunction with previous measurements. Direct comparisons are made with previous predictions by dynamical mean field theory. A general experimental methodology is demonstrated for analogous work on a wide range of strongly correlated f -electron systems.

DOI: [10.1103/PhysRevLett.109.195705](https://doi.org/10.1103/PhysRevLett.109.195705)

PACS numbers: 64.70.K-, 71.10.-w, 71.27.+a, 71.30.+h

Despite decades of work, a coherent, *ab initio* understanding of f electrons in condensed matter remains elusive. Much of this difficulty stems from the nature of both $4f$ and $5f$ states: they exhibit a large density of states near the Fermi energy, are capable of both localized and itinerant character, and often feature multiple low lying quasi-ground states that are nearly degenerate. Accordingly, understanding the electronic interactions that determine the behavior in these systems is challenging. A particularly striking example is elemental Ce metal, which exhibits a large, *isostructural* volume collapse (VC) of $\sim 14\%$ at room temperature terminating in a critical point at ~ 470 K and 1.5 GPa [1,2]. This surprising behavior has allowed the system to serve as a testing ground for state-of-the-art theoretical models treating f -electron correlations. The two latest theoretical models, the Hubbard-Mott (HM) [3] and the Kondo VC (KVC) [4–6] both attempt to explain the evolution of the strongly correlated f electrons across this transition.

Recently, the KVC model has been used to model the experimentally measured equation of state at different temperatures up to 800 K within experimental uncertainty [2]. However, the HM model also seems to be able to reproduce the equation of state in a similar fashion [7] and the matter stands undecided [8,9]. Provocative work in support of the Kondo picture has been performed on Ce alloyed with 10 at. % Sc at 140 K by Murani *et al.* [10]. However, it has been argued that the electron interactions in a 10% alloy are quite different from the pure element and disturb the f electrons, as has been found for other materials [11,12]. Furthermore, the HM model correctly predicts that the transition temperature varies linearly with pressure [13], as experimentally observed [14], while the Kondo model predicts a significant curvature [6]. Also, the

HM model relies on only one adjustable parameter, the ground state energy difference between the two phases [7]. Local density approximation calculations combined with dynamical mean field theory (DMFT) are generally in support of the Kondo screening mechanism for Ce [15–18]. For example, Rueff *et al.* [19] used resonant XES and Anderson impurity model calculations to determine that the number of f electrons (n_f) dropped from 0.97 at 0 kbar to 0.81 at 20 kbar (i.e., across the Ce VC), in general agreement with various DMFT calculations [15,16,20]. Furthermore, DMFT calculations have been expanded to other rare earth elements exhibiting a VC [21], making it very desirable to measure the pure lanthanide metals at high pressure [19,22].

While both KVC and HM theories agree in many aspects, they disagree strongly in their expectations of the behavior of the local $4f$ moment across the VC. The HM model expects the localized $4f$ state of the γ phase to transform into a weakly correlated $4f$ band in the α phase resulting in a quenching of the intrinsic $4f$ moment [3]. On the other hand, the KVC model predicts the onset of dynamic screening of a *stable* $4f$ moment through an exponential rise of the Kondo temperature with decreasing volume, reflected in a rapid drop in entropy from the γ to the α side [15,20]. Though physically quite different, both theories effectively explain the measured differences in the time-averaged magnetic properties of the two phases: the γ phase exhibits paramagnetism of the Curie-Weiss type, and the magnetic susceptibility drops across the VC to values that are more in line with a strongly enhanced Pauli paramagnetism [14,23,24].

Therefore, a measurement of the intrinsic (or instantaneous) magnetic moment per $4f$ electron (i.e., $\langle J \rangle$) can clearly differentiate between the two models. It is this

critical quantity we experimentally investigate, demonstrating that a probe of the *bare* atomic moment ($\langle J \rangle$), in conjunction with previous observations of $4f$ occupation and magnetic susceptibility, provides extremely powerful evidence in the context of the above-discussed debate for Ce. Moreover, as we discuss below, an independent, experimentally determined n_f , though not itself a determination of the moment, contributes an important baseline for interpreting the present results in terms of $\langle J \rangle$. More generally, our approach outlines a methodology that is broadly applicable to many f -electron systems—a class of materials whose complex phase evolutions, often including large VC, have historically been very difficult to understand and predict.

Specifically, this work presents key new evidence, directly validating the KVC model, by combining data from high-pressure nonresonant x-ray emission spectroscopy (NXES) with a modified atomic calculation of elemental Ce. This modified atomic model reproduces the data quite well, allowing us to clearly articulate the meaning of the spectral changes that occur during the VC. We find that the experiment indicates a sudden onset of $4f$ -to-conduction-band hybridization concomitant with the VC, which is consistent with the Kondo hypothesis. More importantly, the experiment shows that in the collapsed phase, there is a persistent instantaneous magnetic moment per $4f$ electron. When coupled with the previously observed drop in magnetic susceptibility over the VC, this persistent moment is compelling evidence of the existence of the Kondo screening mechanism. Finally, we relate our experimental results to explicit, quantitative predictions of the total angular momentum ($\langle J^2 \rangle$) and the number of $4f$ electrons (n_f) made by recent DMFT calculations. Such calculations have enjoyed a spate of recent successes for f -electron materials, such as Ce [19], Pr [22], and Gd [25] as well as actinides such as Pu [26,27] and Am [28,29]. Here, we show that measurements of $\langle J^2 \rangle$ provide a unique and important new benchmark for DMFT implementations.

The Ce $L\gamma$ NXES experiments were performed at beam line 16IDD of the High Pressure Collaborative Access Team (HPCAT) at the Advanced Photon Source. Samples were pressurized through membrane-driven diamond anvil cells and great care was taken to maintain a pure Ce metal sample inside the diamond anvil cells, as reported elsewhere [2,22]. High energy x rays (~ 18 keV) were incident through the diamonds, and the outgoing $L\gamma$ x rays were recorded at 90° to the beam through a 3 mm diam Be gasket by scanning a standard four-inch, spherically bent Si (333) analyzer crystal at 0.25 eV per step with 1 eV resolution.

The spectra were calculated with a treatment specifically developed for this data—a *modified atomic* approach explicitly including the proper atomic physics necessary to describe the deep core-hole spectroscopy [30,31]. Our model for Ce includes the electron-electron interactions

between the $4f$, $3d$, and $2p$ electrons, which are involved in the NXES process as described below but also give rise to, for example, Hund's rules. It is because of these interactions that the $L\gamma$ spectrum has a low-energy satellite feature sensitive to the f -electron occupancy and moment. The f electrons themselves respond to the external applied pressure via their hybridization with higher energy conduction orbitals, but this hybridization is by definition not included in a pure atomic calculation. Therefore, we have extended the local atomic model in analogy with the Anderson impurity model: each of the seven valence f orbitals is allowed to hybridize with five effective conduction orbitals. The number of orbitals included in the calculation (three $2p$, five $3d$, seven $4f$, and five conduction) must remain small because the interactions are treated explicitly via the exact-diagonalization numerical technique, and thus the computational cost increases exponentially with the number of orbitals. Using hybridization to extend the atomic model in this way is similar to the inclusion of explicit ligand atoms, which has proven useful in modeling the spectroscopy of transition-metal and rare-earth oxides in strongly correlated d -electron systems under pressure [32,33]. The parameters of our model are consistent with previous work [6]. We set the $4f$ -orbital energy 0.8 eV below the conduction orbital energy; the hybridization V is varied from 0.0 to 0.2 eV; and the interaction parameters (orbital dependent Coulomb U) are calculated from the Racah parameters given in the output of Cowan's code [34]. The spectra are simulated using the Kramers-Heisenberg formula [35].

In Fig. 1(a), we present the experimental $L\gamma$ NXES data and the predictions from our extended local atomic model, demonstrating that the atomic treatment captures the spectrum quite well. The experiment shows a main emission line near 6052 eV emission energy for the $4d_{3/2} \rightarrow 2p_{1/2}$ transition as well as a satellite feature around 6034 eV. The satellite emanates from a large number of features split into atomic multiplets derived from the electron-electron interactions between the $4f$, $3d$, and $2p$ electrons. The sharpness of the satellite feature in the calculation, compared to the experiment, comes from the fact that the $4f$ electrons are allowed to hybridize with five discrete conduction orbitals, rather than with a broad $5d$ band as in the real metal. The close-up in Fig. 1(c) shows that a steplike decrease in the satellite accompanies the Ce $\gamma \rightarrow \alpha$ VC at ~ 9 kbar in the experimental spectra. Figure 1(c) also shows that this behavior is successfully modeled by the onset of hybridization between the $4f$ orbitals and higher lying d -type states. This yields our first main result: the pressure dependence of the $L\gamma$ spectrum shows $4f$ -to- d hybridization—a key aspect of the Kondo model.

Figure 1(b) demonstrates that the Ce $L\gamma$ measurement is a means of evaluating the *bare* atomic $4f$ moment $\langle J \rangle$. The bare or instantaneous moment is an especially important observable, because in the Kondo picture the $4f$ moments

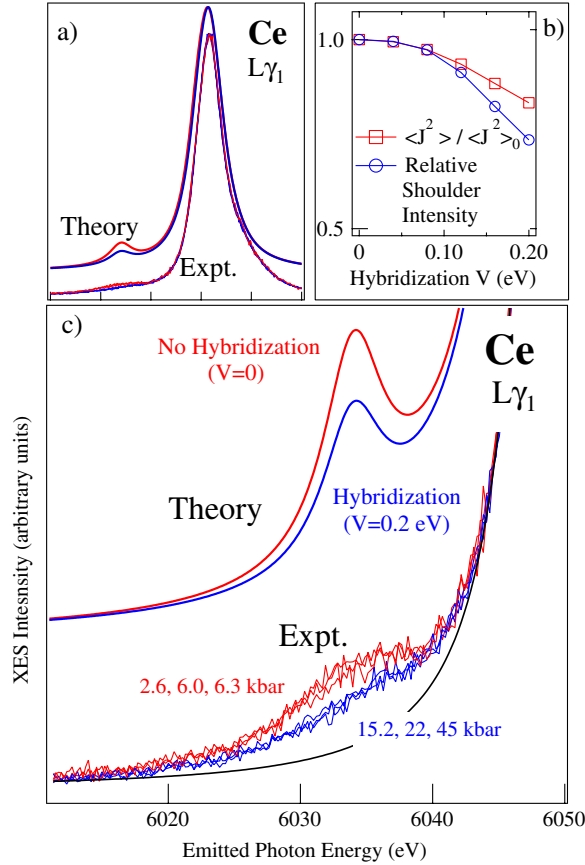


FIG. 1 (color online). (a) The full Ce $L\gamma_1$ emission line as measured experimentally and calculated by the extended atomic model. All theory spectra are shifted by a constant $E_0 = 175$ eV and broadened by convolution with a 5 eV Lorentzian form. (b) Comparison of the calculated shoulder intensity of the $L\gamma_1$ emission line with the instantaneous (*bare*) $\langle J^2 \rangle$ moment. Both decrease with growing hybridization with the shoulder intensity dropping slightly faster than the moment. (c) A close-up of the satellite region revealing the steplike nature of the VC process. The closeup also shows the virtually identical lineshapes for all the pressures below the VC (2.6, 6.0, and 6.3 kbar) and—with a reduced satellite—above the VC (15.2, 22, and 45 kbar). The lines are well fit by a sum of two Lorentzians in the spectral region of interest and the black curve shows the contribution of the main peak in the shoulder region. The calculated spectra with and without hybridization are displayed, showing that this extension outside the atomic limit effectively captures the spectral evolution through the VC.

are dynamically screened by d -band electrons—a mechanism invoked to explain the sharp reduction in the magnetic susceptibility of Ce in the collapsed phase without resorting to fully delocalized $4f$ states, as in the Mott picture [8]. It was expected that the $L\gamma$ x-ray emission measurement would *see* inside the Kondo screening and probe the angular momentum of the atomic-like $4f$ orbitals. In Fig. 1(b), we show that this is indeed confirmed by our calculations: As the f - d hybridization is increased, the satellite intensity and the expected value of the bare atomic

moment (shown in terms of $\langle J^2 \rangle$) are predicted to decrease concurrently. The satellite intensity actually shrinks somewhat faster than the moment. The analogous measurement for transition metal systems, $K\beta$ emission spectroscopy, is commonly used to evaluate $3d$ moments [36,37], and this work opens the door for use of the $L\gamma$ line as an indicator of the bare atomic moment in rare earth materials, via suitable experimental standards.

With this in mind, turning back to the data in Fig. 1(c), we now see that there is a measured decrease in the instantaneous $4f$ moment as Ce progresses through the VC. This puts us in the potentially confusing position of validating the Kondo hypothesis by observing greater f - d mixing, but also observing a lowering of the magnetic moment typically associated with a Mott-like orbital delocalization. The resolution of this apparent conflict lies in considering the number of f electrons per site (n_f) in our enhanced local atomic model, fractional changes of which track fractional changes in the observed moment. As the f - d hybridization parameter is increased, the f electrons are mixed out of their native orbitals and the instantaneous moment drops in proportion to n_f . Put in multiconfigurational language, the $4f^0$ component of the wave function turns on suddenly with the VC, and is weighted more than the $4f^2$ component, which would drive the satellite peak higher. This change in the moment does not indicate a strong change in the $\langle J^2 \rangle$ per $4f$ electron, instead it indicates decreased occupancy, as observed previously [19].

With this understanding of the measurement, it becomes clear that *these results constitute a direct observation of Kondo screening in Ce*: While the magnetic susceptibility is known to drop by $\sim 80\%$ (from 22×10^{-4} to 5×10^{-4} emu/mole) [23,24], the *instantaneous moment* (i.e., $\langle J \rangle$), per $4f$ electron, is here observed to be relatively stable through the collapse. This means the larger drop in susceptibility is not due to intrinsic changes in the $4f$ localization, but is instead a dynamic effect—i.e., the conduction electron screening predicted in the Kondo picture.

We can also make a direct comparison with state-of-the-art dynamical mean-field theory calculations on Ce. To do so, we extract the pressure dependence of the integrated satellite intensity, as shown in Fig. 2. The data points show the satellite intensity with a thick line as a guide for the eye. The sudden change in the satellite is evident at ~ 9 kbar as Ce undergoes the VC transition. The connection to the DMFT calculation is also shown in Fig. 2. As discussed above, both $\langle J^2 \rangle$ and n_f are reflected in the satellite intensity, so previous predictions by DMFT of these quantities are plotted in Fig. 2 as well [21,38]. Fractional changes in the feature intensity, $\langle J^2 \rangle$ and n_f are plotted on the same scale. The size of the change in satellite intensity ($\sim 30\%$) argues that the physics of the volume-collapse transition is dominated by a decrease in n_f , and that any rise in the double occupancy configuration

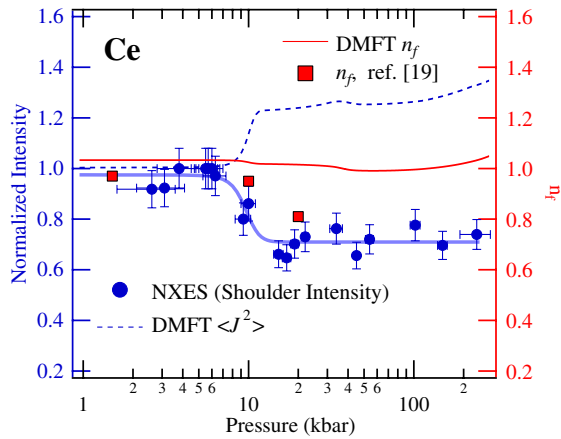


FIG. 2 (color online). Comparison of experimental data with DMFT predictions. Left axis: Comparison of the normalized shoulder intensity (data points with error bars) with predictions for the angular quantum number $\langle J^2 \rangle$ (dashed line), which has been normalized with regard to its atomic value. The predicted $\langle J^2 \rangle$ changes in the opposite direction than does the data. The thick line through the XES data points is a guide for the eye. Right axis: Number of $4f$ electrons n_f . The previous experimental results (large squares) show a drop of 20%, while predicted n_f (solid line) decreases only slightly across the VC. Note that the satellite intensity roughly follows the previous measurement of n_f , with the drop in intensity being slightly larger. The modified atomic calculations predict this greater drop in satellite intensity in comparison to n_f , just as they do in comparison to $\langle J^2 \rangle$, as shown in Fig. 1(b).

is relatively minor. This is in contrast to current DMFT calculations, which predict a significant rise in the bare magnetic moment due to growth in the double-occupancy configuration [21,38], as shown here. DMFT, however, has been successful in predicting a large decrease in the *screened* moment [38] comparable to the collapse of the magnetic susceptibility measured experimentally [23,24]. The high temperature (632 K) required for the current DMFT calculations could affect the calculated f electron count, and furthermore, other implementations of DMFT predict a greater drop in n_f for Ce over the VC [11,19], so better agreement in terms of may be possible. Regardless, the issue can now be addressed because this experimental benchmark is available.

In conclusion, we have presented experimental results from high-pressure NXES on elemental Ce metal, along with a new, modified-atomic treatment to simulate the spectra. This experiment-theory combination allows us to present strong support of the Kondo hypothesis for the Ce isostructural ($\gamma - \alpha$) VC transition. In addition to dealing with this specific, long-argued scientific question, this work also contributes within the larger context of strongly-correlated condensed-matter physics by (i) providing an important new benchmark for DMFT predictions and (ii) exhibiting a program of study relevant for many f -electron systems, where effective experimental method-

ologies are sorely needed to unravel the difficult general issue of f -electron (de)localization and its effects on material properties.

This work has been supported by the LDRD 07-ERD-029 and 12-LW-014 at LLNL and was performed under the auspices of the U.S. Department of Energy by Lawrence Livermore National Laboratory in part under Contract No. W-7405-Eng-48 and in part under Contract No. DE-AC52-07NA27344. The x-ray work was performed at beam line 16IDD of the HPCAT at the Advanced Photon Source (APS), Argonne National Laboratory. HPCAT is supported by CIW, CDAC, UNLV and LLNL through funding from DOE-NNSA, DOE-BES and NSF. APS is supported by DOE-BES, under Contract No. DE-AC02-06CH11357. T.P.D. and A.P.S. were supported by the U.S. DOE under Contract No. DE-AC02-76SF00515. The authors would like to thank A.K. McMahan for a critical reading of an earlier manuscript and many very valuable discussions and suggestions.

*Corresponding author: bradley41@llnl.gov

- [1] F. Decremps, L. Belhadi, D.L. Farber, K.T. Moore, F. Ocelli, M. Gauthier, A. Polian, D. Antonangeli, C.M. Aracne-Ruddle, and B. Amadon, *Phys. Rev. Lett.* **106**, 065701 (2011).
- [2] M.J. Lipp, D. Jackson, H. Cynn, C. Aracne, W.J. Evans, and A.K. McMahan, *Phys. Rev. Lett.* **101**, 165703 (2008).
- [3] B. Johansson, *Philos. Mag.* **30**, 469 (1974); *Phys. Rev. B* **11**, 2740 (1975).
- [4] J.W. Allen and R.M. Martin, *Phys. Rev. Lett.* **49**, 1106 (1982).
- [5] M. Lavagna, C. Lacroix, and M. Cyrot, *Phys. Lett.* **90A**, 210 (1982).
- [6] J.W. Allen and L.Z. Liu, *Phys. Rev. B* **46**, 5047 (1992).
- [7] B. Johansson, A.V. Ruban, and I.A. Abrikosov, *Phys. Rev. Lett.* **102**, 189601 (2009).
- [8] G. Kotliar, S.Y. Savrasov, K. Haule, V.S. Oudovenko, O. Parcollet, and C.A. Marianetti, *Rev. Mod. Phys.* **78**, 865 (2006).
- [9] K.T. Moore and G. van der Laan, *Rev. Mod. Phys.* **81**, 235 (2009).
- [10] A.P. Murani, S.J. Levett, and J.W. Taylor, *Phys. Rev. Lett.* **95**, 256403 (2005).
- [11] J.-P. Rueff, *Rev. Mod. Phys.* **82**, 847 (2010).
- [12] E. Vescovo, L. Braicovich, B. De Michelis, A. Fasana, R. Eggenhöfner, G. Iandelli, G.L. Olcese, and A. Palenzona, *Phys. Rev. B* **43**, 12281 (1991).
- [13] B. Johansson, I.A. Abrikosov, M. Aldén, A.V. Ruban, and H.L. Skriver, *Phys. Rev. Lett.* **74**, 2335 (1995).
- [14] D.C. Koskenmaki and K.A. Gschneidner, Jr., *Handbook on the Physics and Chemistry of Rare Earths* (North-Holland, Amsterdam, 1978), Chap. 4, p. 337.
- [15] A.K. McMahan, K. Held, and R.T. Scalettar, *Phys. Rev. B* **67**, 075108 (2003).
- [16] M.B. Zöfll, I.A. Nekrasov, T. Pruschke, V.I. Anisimov, and J. Keller, *Phys. Rev. Lett.* **87**, 276403 (2001).

- [17] K. Held, A. K. McMahan, and R. T. Scalettar, *Phys. Rev. Lett.* **87**, 276404 (2001).
- [18] K. Haule, V. Oudovenko, S. Y. Savrasov, and G. Kotliar, *Phys. Rev. Lett.* **94**, 036401 (2005).
- [19] J.-P. Rueff, J.-P. Itie, M. Taguchi, C.F. Hague, J.-M. Mariot, R. Delaunay, J.-P. Kappler, and N. Jaouen, *Phys. Rev. Lett.* **96**, 237403 (2006).
- [20] B. Amadon, S. Biermann, A. Georges, and F. Aryasetiawan, *Phys. Rev. Lett.* **96**, 066402 (2006).
- [21] A. K. McMahan, *Phys. Rev. B* **72**, 115125 (2005).
- [22] J. A. Bradley, K. T. Moore, M. J. Lipp, B. A. Mattern, J. I. Pacold, G. T. Seidler, P. Chow, E. Rod, Y. Xiao, and W. J. Evans, *Phys. Rev. B* **85**, 100102 (2012).
- [23] M. R. MacPherson, G. E. Everett, D. Wohlleben, and M. B. Maple, *Phys. Rev. Lett.* **26**, 20 (1971).
- [24] T. Naka, T. Matsumoto, and N. Mori, *Physica (Amsterdam)* **205B**, 121 (1995).
- [25] B. R. Maddox, A. Lazicki, C. S. Yoo, V. Iota, M. Chen, A. K. McMahan, M. Y. Hu, P. Chow, R. T. Scalettar, and W. E. Pickett, *Phys. Rev. Lett.* **96**, 215701 (2006).
- [26] X. Dai, S. K. Savrasov, G. Kotliar, A. Migliori, H. Ledbetter, and E. Abrahams, *Science* **300**, 953 (2003).
- [27] J. H. Shim, K. Haule, and G. Kotliar, *Nature (London)* **446**, 513 (2007).
- [28] J.-C. Griveau, J. Rebizant, G. H. Lander, and G. Kotliar, *Phys. Rev. Lett.* **94**, 097002 (2005).
- [29] S. Y. Savrasov, K. Haule, and G. Kotliar, *Phys. Rev. Lett.* **96**, 036404 (2006).
- [30] F. de Groot and A. Kotani, *Core Level Spectroscopy of Solids* (CRC Press, Boca Raton, 2008).
- [31] J. S. Griffith, *The Theory of Transition-Metal Ions* (Cambridge University Press, Cambridge, England, 1971).
- [32] S. Wang, W. L. Mao, A. P. Sorini, C.-C. Chen, T. P. Devereaux, Y. Ding, Y. Xiao, P. Chow, N. Hiraoka, H. Ishii, Y. Q. Cai, C.-C. Kao, *Phys. Rev. B* **82**, 144428 (2010).
- [33] W. S. Lee, A. P. Sorini, M. Yi, Y. D. Chuang, B. Moritz, W. L. Yang, J.-H. Chu, H. H. Kuo, A. G. Cruz-Gonzalez, I. R. Fisher, Z. Hussain, T. P. Devereaux, and Z. X. Shen, *Phys. Rev. B* **85**, 155142 (2012).
- [34] R. D. Cowan, *The Theory of Atomic Structure and Spectra* (University of California Press, Berkeley, 1981).
- [35] W. Schuelke, *Electron Dynamics by Inelastic X-Ray Scattering* (Oxford University Press, New York, 2007).
- [36] F. de Groot, *Chem. Rev.* **101**, 1779 (2001).
- [37] G. Peng, F. M. F. de Groot, K. Hamalainen, J. A. Moore, X. Wang, M. M. Grush, J. B. Hastings, D. P. Siddons, W. H. Armstrong, O. C. Mullins, and S. P. Cramer, *J. Am. Chem. Soc.* **116**, 2914 (1994).
- [38] A. K. McMahan, R. T. Scalettar, and M. Jarrell, *Phys. Rev. B* **80**, 235105 (2009).